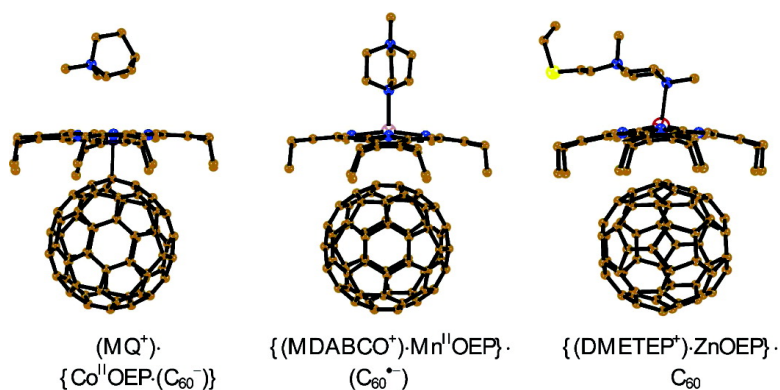


Design of Molecular and Ionic Complexes of Fullerene C with Metal(II) Octaethylporphyrins, MOEP (M = Zn, Co, Fe, and Mn) Containing Coordination M#N(ligand) and M#C(C) Bonds

Dmitri V. Konarev, Salavat S. Khasanov, Gunzi Saito, and Rimma N. Lyubovskaya

Cryst. Growth Des., **2009**, 9 (2), 1170-1181 • DOI: 10.1021/cg8010184 • Publication Date (Web): 29 December 2008

Downloaded from <http://pubs.acs.org> on February 12, 2009



More About This Article

Additional resources and features associated with this article are available within the HTML version:

- Supporting Information
- Access to high resolution figures
- Links to articles and content related to this article
- Copyright permission to reproduce figures and/or text from this article

[View the Full Text HTML](#)



Design of Molecular and Ionic Complexes of Fullerene C₆₀ with Metal(II) Octaethylporphyrins, M^{II}OEP (M = Zn, Co, Fe, and Mn) Containing Coordination M–N(ligand) and M–C(C₆₀[−]) Bonds

Dmitri V. Konarev,^{*,†} Salavat S. Khasanov,[‡] Gunzi Saito,[§] and Rimma N. Lyubovskaya[†]

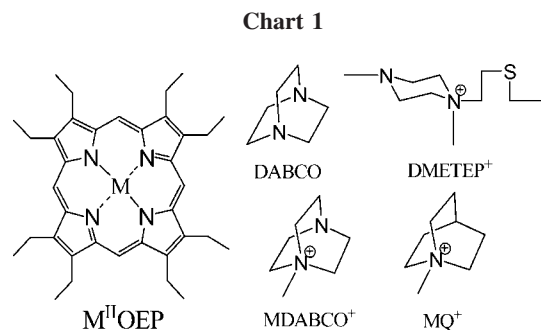
Institute of Problems of Chemical Physics RAS, Chernogolovka, Russia, Institute of Solid State Physics RAS, Chernogolovka, Moscow Region, 142432, Russia, and Division of Chemistry, Graduate School of Science, Kyoto University, Sakyo-ku, Kyoto 606-8502, Japan

Received September 11, 2008; Revised Manuscript Received November 5, 2008

ABSTRACT: The formation of coordination bonds between metalloporphyrins and *N*-containing ligands or C₆₀[−] was used to prepare molecular and ionic complexes of C₆₀ with metal(II) octaethylporphyrins: {M^{II}OEP·DABCO}·C₆₀·(Solvent) (M = Zn (**4**) and Co (**5**)); {(MDABCO⁺)·M^{II}OEP}·(C₆₀[−])·(Solvent) (M = Zn (**6**), Fe (**8**), and Mn (**9**)), (MQ⁺)·{Co^{II}OEP·(C₆₀[−])}·C₆H₄Cl₂ (**10**) and {(DMETEP⁺)·Zn^{II}OEP}·(C₆₀[−])·(C₆₀)_{0.5}·C₆H₄Cl₂ (**12**). New molecular complexes of C₆₀ with ligand free metalloporphyrins M^{II}OEP·C₆₀·(Solvent)_{1.5} (M = Zn (**1**), Co (**2**), and Fe (**3**)) were also obtained for comparison. Complexes **1–3** contain alternating pairs of C₆₀ and M^{II}OEP molecules, whereas isostructural complexes **4–10** contain porphyrin channels accommodating zigzag fullerene species arranged in zigzag chains and cavities formed by two (DMETEP⁺)·ZnOEP units. The coordination of DABCO, MDABCO⁺, DMETEP⁺, C₆₀, and C₆₀[−] to M^{II}OEP was studied and their coordination abilities were compared. C₆₀ weakly coordinates to Fe^{II}OEP and Co^{II}OEP porphyrins with rather short M···C(C₆₀) distances of 2.622 Å (**3**) and 2.685 Å (**2**). Only one *N*-containing ligand (L or L⁺) coordinates to M^{II}OEP in **4–9** and **12** to form five-coordinated L(L⁺)·M^{II}OEP species with the M···N(L or L⁺) bond lengths of 2.18–2.39 Å. These bonds are shorter by 0.049–0.055 Å for DABCO than for the MDABCO⁺ cation, and by 0.214 Å than for the DMETEP⁺ cation. Fullerenes are located from the opposite side of the porphyrin macrocycle relative to L (L⁺). They are essentially weaker ligands than L (L⁺) and form M···C(C₆₀ or C₆₀[−]) distances longer than 2.84 Å. Neutral complex **3** with Fe^{II}OEP in intermediate (*S* = 1) spin state manifests a Weiss temperature of 2.6 K. C₆₀[−] coexists with diamagnetic Zn^{II}OEP in **6** and high-spin Fe^{II}OEP and Mn^{II}OEP in **8** and **9**. The Weiss temperatures of −17.8, −42.0, and −2.5 K, respectively, indicate antiferromagnetic coupling of spins in these complexes. The MQ⁺ cation is not coordinated to Co^{II}OEP in **10** providing the formation of stable Co–C(C₆₀[−]) coordination bonds of 2.266(3) Å length and diamagnetism of the complex.

Fullerenes form a variety of molecular and ionic complexes with different types of organic and organometallic donors.¹ Among them, fullerene complexes with metalloporphyrins² attract special attention since flexible porphyrin molecules are able to form complexes not only with fullerenes² but with a variety of endometallofullerenes and chemically modified fullerenes.^{2a,3} That allows one to investigate molecular and electronic structures of new families of fullerenes. Design of ionic fullerene complexes with metalloporphyrins is a promising approach to study fullerenes in a charged state.⁴ In the future, that can allow one to study the anions of endometallofullerenes and chemically modified fullerenes. Since fullerene anions have a strong tendency to form interfullerene σ -bonds, another interesting possibility of this approach is the preparation of new σ -bonded structures from negatively charged fullerenes such as dimers and polymers.^{4b–d} Coordination of fullerene anions to metalloporphyrins can also be realized. Now there are only a few examples of such coordination.^{4e,f}

Since fullerenes are relatively weak acceptors (as compared with planar π -acceptors tetracyanoethylene or tetracyanoquinodimethane),⁵ most of fullerene complexes with metalloporphyrins have only a neutral ground state.² We developed new approaches to prepare ionic fullerene–porphyrin complexes which use relatively weak coordination bonding between metalloporphyrins and *N*-containing ligands (cations) (the M–N(L) bonds) or fullerene radical anions (the M–C(C₆₀[−])



bonds). For example, bidentate ligands such as 4,4'-bipyridine (BPY) and *N,N'*-dimethylpiperazine (DMP) bind metalloporphyrins in binuclear structures which can cocrystallize with fullerenes to form ionic complexes: {(ZnOEP)₂·BPY}·(TDAE⁺⁺)·(C₆₀[−])·(Solvent)_x^{4a} and {(Mn^{II}TPP)₂·DMP}·(DMETEP⁺)₂·(C₆₀[−])₂·(Solvent)_x^{4b} (OEP is octaethylporphyrin; TDAE is tetrakis(dimethylamino)ethylene; TPP is tetraphenylporphyrin; DMETEP⁺ is the *N,N'*-dimethyl-*N'*-ethylthioethylpiperazinium cation (Chart 1)). The *N*-methylidiazabicyclooctane cation (MDABCO⁺, Chart 1) has a free nitrogen atom and coordinates to different metalloporphyrins (M = Zn, Co^{II}, Fe^{II}, and Mn^{II}). Since MDABCO⁺ can be a countercation for fullerene anions, neutral metalloporphyrin molecules are involved in the ionic complexes with fullerenes as positively charged coordination assemblies: {(MDABCO⁺)·M^{II}porphyrin}·(C₆₀[−])_n (*n* = 1 and 2). The obtained complexes contain unusual (C₆₀[−])₂ dimers bonded by two single bonds in {(MDABCO⁺)·Co^{II}TMPP}₂·(C₆₀[−])₂·(Solvent)_x^{4c} (TMPP is tetrakis(4-methoxyphenyl)porphyrin),

* To whom correspondence should be addressed. E-mail: konarev@icp.ac.ru.

[†] Institute of Problems of Chemical Physics RAS.

[‡] Institute of Solid State Physics RAS.

[§] Kyoto University.

antiferromagnetically coupled C₆₀^{•-} chains and diamagnetic (C₇₀)₂ dimers in the {(MDABCO⁺)₂·M^{III}TTPP}·(C₆₀₍₇₀₎)₂·(Solvent)_x complexes (M = Zn, Co, Mn, and Fe).^{4d}

Neutral metalloporphyrin molecules can also be involved in the ionic fullerene complexes when coordination bonds are formed between fullerene radical anions and cobalt(II) tetraphenyl- or octaethylporphyrins. In this case neutral metalloporphyrin molecules are involved in the ionic complex as negatively charged coordination assembly: (C⁺)·{Co^{II}TTPP·(C₆₀⁻)}·(Solvent)_x (C⁺ is the cation of bis(benzene)chromium (Cr^I(C₆H₆)₂^{•+})^{4e} or TDAE^{•+})^{4f} and (TMP⁺)·{Co^{II}OEP·(C₆₀⁻)}·(Solvent)_x (TMP⁺ is the tetramethylphosphonium cation).^{4g} The Co–C coordination bonds in these complexes have a length of 2.28–2.32 Å and the resulting {Co^{II}porphyrin·(C₆₀⁻)} coordination assemblies are diamagnetic.^{4e–4g} The Co–C(C₆₀⁻) coordination bonds were reversibly formed in the {(MDABCO⁺)·Co^{II}OEP}·(C₆₀⁻) coordination units resulted in the transition of the complex from paramagnetic to diamagnetic state.^{4g}

In this work we studied new coordination architectures of M^{II}OEP (Chart 1) with neutral and cationic *N*-containing ligands which were further cocrystallized with fullerenes. Since fullerenes can be in neutral or anionic form, this method is suitable for the preparation of various molecular and ionic complexes. Those are C₆₀ complexes with diazabicyclooctane (DABCO, Chart 1)) coordinated porphyrins (M = Zn and Co); C₆₀^{•-} complexes with porphyrins coordinated MDABCO⁺ (M = Zn, Fe, and Mn) or DMETEP⁺ cations (M = Zn) and (MQ⁺)·{Co^{II}OEP·(C₆₀⁻)}·(Solvent)_x complex containing noncoordinating *N*-methylquinuclidinium cations (MQ⁺, Chart 1). New molecular complexes of C₆₀ with ligand free metalloporphyrins (M = Zn, Co, and Fe) were also obtained for comparison. Crystal structures of nine complexes were studied. The complexes were characterized by the spectra in the UV–visible–NIR and IR-ranges, EPR and temperature dependent magnetic measurements down to 1.9 K. Structures, optical and magnetic properties of the complexes were discussed. Different coordination modes of neutral and cationic *N*-containing ligands, fullerenes and fullerene radical anions to metalloporphyrins were studied and their coordination abilities were compared. For the first time the effect of positive charge of ligand on the M–N(L) bonds length was found. Molecular structures, optical properties and spin state of metal(II) octaethylporphyrins in new neutral and positively charged coordination assemblies were investigated for the first time.

Experimental Section

Materials. Zinc(II) octaethylporphyrin (ZnOEP), cobalt(II) octaethylporphyrin (Co^{II}OEP), manganese(III) octaethylporphyrin chloride (Mn^{III}OEP·Cl), iron (III) octaethylporphyrin chloride (Fe^{III}OEP·Cl), NaBH₄, diazabicyclooctane (DABCO), quinuclidine, sodium ethanethiolate (CH₃CH₂SNa), methyl iodide (CH₃I) were purchased from Aldrich. C₆₀ of 99.98% purity was received from MTR Ltd. Solvents were purified in argon atmosphere. *o*-Dichlorobenzene (C₆H₄Cl₂) was distilled over CaH₂ under reduced pressure, benzonitrile (C₆H₅CN) was distilled over Na under reduced pressure, and hexane was distilled over Na/benzophenone. The solvents were degassed and stored in a glovebox. All manipulations for the synthesis of air-sensitive **3**, **6**, **8–10**, and **12** were carried out in a MBraun 150B-G glovebox with controlled atmosphere and the content of H₂O and O₂ less than 1 ppm. The crystals were stored in a glovebox and sealed in anaerobic conditions in 2 mm quartz tubes for EPR and SQUID measurements under 10⁻⁵ Torr. KBr pellets for IR- and UV–visible–NIR measurements were prepared in a glovebox.

Synthesis. *N*-Methyldiazabicyclooctane iodide (MDABCO·I) and *N,N'*-dimethyldiazabicyclooctane diiodide (DMDABCO·I₂) were obtained as described previously.^{4g,b} *N*-Methylquinuclidine iodide (MQ·I)

was prepared similarly. Quinuclidine (1 g, 0.01 mol) was dissolved in 50 mL of hexane. CH₃I (1 mL, 0.016 mol) was slowly added to the obtained solution upon intensive stirring. A white crystalline precipitate of MQ·I began to form immediately. After 1 h the precipitate was filtered off, washed with 50 mL of hexane, and dried in a vacuum for 4 h. Two grams of MQ·I was obtained with 90% yield and satisfactory elemental analysis.

Iron(II) and manganese(II) octaethylporphyrins were obtained by the reduction of M^{III}OEP·Cl with NaBH₄ in anaerobic conditions. About 30 mg of NaBH₄ was dissolved in 3 mL of warm ethanol. The solution was cooled down to room temperature and filtered. One-hundred milligrams of M^{III}OEP·Cl was added to the obtained solution. The reduction was carried out for 24 h. M^{II}OEP precipitated from solution. The precipitate was filtered off, washed with ethanol (2 mL), and dried to give Fe^{II}OEP and Mn^{II}OEP with 50–70% yield.

The synthesis of {(MDABCO⁺)·Co^{II}OEP}·(C₆₀^{•-})·(C₆H₅CN)_{0.67}·(C₆H₄Cl₂)_{0.33} (**7**) and (TMP⁺)·{Co^{II}OEP·(C₆₀⁻)}·(C₆H₅CN)_{0.75}·(C₆H₄Cl₂)_{0.25} (**11**) was described previously.^{4g} The crystals of **1–6**, **8–10**, and **12** were obtained by evaporation or diffusion as black prisms with characteristic blue luster (up to 1 × 1 × 0.5 mm³ in size) with 50–80% yield. In all cases the formation of C₆₀^{•-} radical anions at the reduction was justified by the NIR spectra of the solutions. The diffusion was carried out during one month in a glass tube of 1.8 cm diameter and 50 mL volume with a ground glass plug. After the diffusion finished the solvent was decanted from the crystals and they were washed with hexane.

The crystals of ZnOEP·C₆₀·(C₆H₄Cl₂)_{1.5} (**1**) were obtained by diffusion of hexane (25 mL) in C₆H₄Cl₂ solution containing C₆₀ (25 mg, 0.035 mmol) and one molar equivalent of ZnOEP (20.6 mg, 0.035 mmol).

Diffusion of CHCl₃ solution of Co^{II}OEP (20.6 mg, 0.035 mmol) into C₆H₅Cl solution of C₆₀ (25 mg, 0.035 mmol) gave the crystals of known phase of orthorhombic (Co^{II}OEP)₂·C₆₀·CHCl₃.^{2a} The crystals of Co^{II}OEP·C₆₀·(C₆H₅Cl)_{1.5} (**2**) were obtained by slow evaporation of the resulting solution in argon atmosphere for a week. The crystals were washed with acetone.

Polycrystalline Fe^{II}OEP·C₆₀·(C₆H₄Cl₂)_{1.5} (**3**) was obtained by slow diffusion of hexane into a C₆H₄Cl₂/C₆H₅CN (14:2) mixture containing C₆₀ (25 mg, 0.035 mmol) and one molar equivalent of Fe^{II}OEP (20.6 mg, 0.035 mmol). However, high-quality single crystals of **3** were obtained when we tried to synthesize ionic (MQ⁺)·Fe^{II}OEP·(C₆₀^{•-}) complex. C₆₀ (25 mg, 0.035 mmol), a 10-fold molar excess of CH₃CH₂SNa (30 mg, 0.36 mmol) and a 5-fold molar excess of MQ·I (44 mg, 0.175 mmol) were stirred in the C₆H₄Cl₂/C₆H₅CN (14:2) mixture for 2 h at 60 °C. The solution was cooled down to room temperature (RT = 295 K) and filtered, Fe^{II}OEP (20.5 mg, 0.035 mmol) was dissolved and 25 mL of hexane was layered over the obtained solution. Diffusion yielded several well-shaped crystals of **3** grown in a hexane part of the diffusion cell (yield 5%), whereas the desired ionic complex was not formed. Complex **3** obtained by both methods showed the same IR, UV–vis–NIR, and EPR spectra.

The crystals of {ZnOEP·DABCO}·C₆₀·(C₆H₅CN)_{0.3}·(C₆H₄Cl₂)_{0.7} (**4**) were obtained by the diffusion of hexane into the C₆H₄Cl₂/C₆H₅CN (14:2) solution containing C₆₀ (25 mg, 0.035 mmol), one molar equivalent of ZnOEP (20.6 mg, 0.035 mmol), and an excess of DABCO (100 mg, 0.893 mmol). The obtained crystals were washed with hexane.

The crystals of {Co^{II}OEP·DABCO}·C₆₀·C₆H₅Cl (**5**) were obtained by the diffusion of CHCl₃ solution (25 mL) containing Co^{II}OEP (20.6 mg, 0.035 mmol) and an excess of DABCO (100 mg, 0.893 mmol) into the C₆H₅Cl solution (15 mL) containing C₆₀ (25 mg, 0.035 mmol). The crystals of **5** were washed with acetone.

The crystals of {(MDABCO⁺)·ZnOEP}·(C₆₀^{•-})·(C₆H₅CN)_{0.75}·(C₆H₄Cl₂)_{0.25} (**6**), {(MDABCO⁺)·Fe^{II}OEP}·(C₆₀^{•-})·(C₆H₅CN)_{0.4}·(C₆H₄Cl₂)_{0.6} (**8**), and {(MDABCO⁺)·Mn^{II}OEP}·(C₆₀^{•-})·(C₆H₅CN)_{0.88}·(C₆H₄Cl₂)_{0.12} (**9**) were obtained by diffusion. C₆₀ (25 mg, 0.035 mmol), a 10-fold molar excess of CH₃CH₂SNa (30 mg, 0.36 mmol) and a 5-fold molar excess of MDABCO·I (44.5 mg, 0.175 mmol) were stirred in the C₆H₄Cl₂/C₆H₅CN (14:2) mixture for 2 h at 60 °C. The solution was cooled down to RT and filtered, ZnOEP (**6**), Fe^{II}OEP (**8**), or Mn^{II}OEP (**9**) (~21 mg, 0.035 mmol) were dissolved and 25 mL of hexane was layered over the obtained solution. The diffusion yielded the crystals of **6**, **8**, and **9** as a single phase.

The crystals of (MQ⁺)·{Co^{II}OEP·(C₆₀⁻)}·C₆H₄Cl₂ (**10**) were obtained by diffusion. C₆₀ (25 mg, 0.035 mmol), a 10-fold molar excess of CH₃CH₂SNa (30 mg, 0.36 mmol) and a 5-fold molar excess of MQ·I

Chart 2

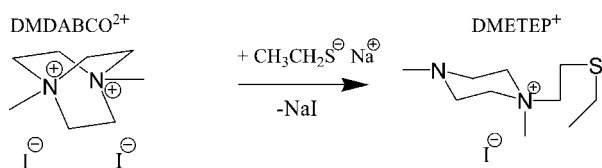


Table 1. Compositions of the Complexes

N	composition of the complex			ref
	porphyrin unit	fullerenes	solvent	
1	ZnOEP•	C ₆₀ •	(C ₆ H ₄ Cl ₂) _{1.5}	
2	Co ^{II} OEP•	C ₆₀ •	(C ₆ H ₅ Cl) _{1.5}	
3	Fe ^{II} OEP•	C ₆₀ •	(C ₆ H ₄ Cl ₂) _{1.5}	
4	{ZnOEP•DABCO}•	C ₆₀ •	(C ₆ H ₅ CN) _{0.7} •(C ₆ H ₄ Cl ₂) _{0.3}	
5	{Co ^{II} OEP•DABCO}•	C ₆₀ •	C ₆ H ₅ Cl	
6	{(MDABCO ⁺)•ZnOEP}•	(C ₆₀ ⁻)•	(C ₆ H ₅ CN) _{0.75} •(C ₆ H ₄ Cl ₂) _{0.25}	
7	{(MDABCO ⁺)•Co ^{II} OEP}•	(C ₆₀ ⁻)•	(C ₆ H ₅ CN) _{0.67} •(C ₆ H ₄ Cl ₂) _{0.33}	4g
8	{(MDABCO ⁺)•Fe ^{II} OEP}•	(C ₆₀ ⁻)•	(C ₆ H ₅ CN) _{0.4} •(C ₆ H ₄ Cl ₂) _{0.6}	
9	{(MDABCO ⁺)•Mn ^{II} OEP}•	(C ₆₀ ⁻)•	(C ₆ H ₅ CN) _{0.88} •(C ₆ H ₄ Cl ₂) _{0.12}	
10	(MQ ⁺)•(Co ^{II} OEP)•	C ₆₀ ⁻ •	C ₆ H ₄ Cl ₂	
11	(TMP ⁺)•(Co ^{II} OEP)•	C ₆₀ ⁻ •	(C ₆ H ₅ CN) _{0.75} •(C ₆ H ₄ Cl ₂) _{0.25}	4g
12	{(DMETEP ⁺)•ZnOEP}•	(C ₆₀ ⁻)•(C ₆₀) _{0.5}	C ₆ H ₄ Cl ₂	

(44 mg, 0.175 mmol) were stirred in the C₆H₄Cl₂/C₆H₅CN (14:2) mixture for 2 h at 60 °C. The solution was cooled down to RT and filtered, Co^{II}OEP (20.5 mg, 0.035 mmol) was dissolved and 25 mL of hexane was layered over the obtained solution. The diffusion yielded the crystals of **10** as a single phase. The use of Mn^{II}OEP, Fe^{II}OEP, and ZnOEP instead of Co^{II}OEP did not yield desired crystals of ionic complexes.

The crystals of {(DMETEP⁺)•ZnOEP}•(C₆₀⁻)•(C₆₀)_{0.5}•C₆H₄Cl₂ (**12**) were obtained by diffusion. C₆₀ (25 mg, 0.035 mmol), a 10-fold molar excess of CH₃CH₂SNa (30 mg, 0.36 mmol) and a 4-fold molar excess of DMDABCO•I₂ (44.5 mg, 0.175 mmol) were stirred in the C₆H₄Cl₂/C₆H₅CN (14:2) mixture for 2 h at 60 °C. The solution was cooled down to RT and filtered, ZnOEP (21 mg, 0.035 mmol) was dissolved and 25 mL of hexane was layered over the obtained solution. The diffusion yielded the crystals of **12**. The composition of **12** was determined from X-ray diffraction studies on a single crystal (several crystals from the synthesis were tested). Even though the starting cation was DMDABCO²⁺, another DMETEP⁺ cation was found in the structure of **12**. Most probably in contrast to the MDABCO⁺ cation, which was stable in the presence of CH₃CH₂S⁻, DMDABCO²⁺ was unstable. The reaction is realized through a nucleophilic addition of CH₃CH₂S⁻ to one of the positively charged nitrogen atoms of DMDABCO²⁺, one C–N⁺ bond opens, one new C–S bond forms and the DMDABCO²⁺ dication transforms to the DMETEP⁺ cation (Chart 2). Namely, the DMETEP⁺ cation was previously found in the {(Mn^{II}TPP)₂•DMP}•(DMETEP⁺)₂•(C₆₀⁻)₂•(Solvent)_x complex synthesized starting from DMDABCO•I₂.^{4b}

The composition of **1–6**, **9**, **10**, and **12** was determined from X-ray structural analysis on single crystal (Table 1). Careful examination of the crystals under the microscope and tests of several crystals from the synthesis by X-ray diffraction showed them to belong to one crystal phase. The crystals of **8** were small in size for the X-ray diffraction experiment and the composition of this complex was determined from the elemental analysis: C₁₀₉H_{63.4}N_{6.4}O₄Cl_{1.2}Fe (1624.69); found, %: C = 79.39, H = 3.87, N = 5.28; Cl = 2.59; calc., %: C = 80.58, H = 3.91, N = 5.52; O = 3.95; Cl = 2.62; Fe = 3.45. The difference between the value calculated from the expression (100, % - (found content of C, H, N, Cl), %) and the calculated content of Fe for **8** indicated the addition of oxygen to the complex in the course of analysis (about two O₂ molecules per formula unit, which contains air-sensitive Fe^{II}OEP and C₆₀⁻). The addition of O₂ to ionic C₆₀ complexes during the elemental analysis was reported.⁶

General. UV–visible–NIR spectra were measured in KBr pellets on a Shimadzu-3100 spectrometer in the 240–2600 nm range. FT-IR spectra were measured in KBr pellets with a Perkin-Elmer 1000 Series spectrometer (400–7800 cm⁻¹). EPR spectra were recorded from 295 down to 4 K with a JEOL JES-TE 200 X-band ESR spectrometer equipped with a JEOL ES-CT470 cryostat. A Quantum Design MPMS-XL SQUID magnetometer was used to measure static susceptibilities

of polycrystalline **3**, **6**, **8–10** between 300 and 1.9 K in a 100 mT static magnetic field. A sample holder contribution and core temperature independent diamagnetic susceptibility (χ_0) were subtracted from the experimental values. The values of C , Θ , and χ_0 were calculated in a high-temperature range using the formula: $\chi_M = C/(T - \Theta) + \chi_0$. Effective magnetic moments of the complexes were calculated using the formula: $\mu_{\text{eff}} = (8 \cdot \chi_M \cdot T)^{1/2}$.

Crystal Structure Determination. X-ray diffraction data for **1–6**, **9–10**, and **12** are listed in Table 2. The intensity data for **5**, **9–10**, and **12** were collected on a MAC Science DIP-2020K oscillator type X-ray imaging plate diffractometer with graphite monochromated Mo K α radiation at low temperatures using an Oxford Cryostream cooling system. Raw data reduction to F^2 was carried out using the DENZO program.⁷ X-ray diffraction data for **1–4** and **6** were collected using a Bruker Nonius X8 Apex diffractometer with a CCD area detector (Mo K α radiation, $\lambda = 0.71073$ Å) equipped with an Oxford Cryosystems nitrogen gas-flow apparatus. The data were collected by φ and ω -scans with 0.3° frame-width and 30 s exposure time per frame. The data were integrated, scaled, sorted, and averaged using the Bruker AXS software package.⁸ The structures were solved by direct method and refined by the full-matrix least-squares method against F^2 using SHELX-97.⁹ Non-hydrogen atoms were refined in the anisotropic approximation. Positions of hydrogen atoms were calculated geometrically. Subsequently, the positions of H atoms were refined by the “riding” model with $U_{\text{iso}} = 1.2U_{\text{eq}}$ of the connected non-hydrogen atom or as ideal CH₃ groups with $U_{\text{iso}} = 1.5U_{\text{eq}}$.

Molecular Disorder in 1–6 and 9–10. C₆₀ molecules are disordered in **1** between two orientations with the 0.88/0.12 occupancies. The orientations are linked by the rotation of the C₆₀ molecule by 180° about a 3-fold axis passing through the centers of two oppositely located hexagons. There are two positions of C₆H₄Cl₂ molecules. They are ordered in the fully occupied position, whereas they are disordered between two orientations in the 50% occupied position.

C₆₀ molecules are ordered in **2**. The C₆H₅Cl molecules occupy two positions. In a fully occupied position, they are disordered between two orientations with the 0.835/0.165 occupancies, whereas in the 50% occupied position they are statistically disordered between two orientations.

There are two crystallographically independent C₆₀ and Fe^{II}OEP molecules in **3**. Both C₆₀ molecules are disordered between two orientations with the 0.74/0.26 and 0.73/0.27 occupancies. C₆H₄Cl₂ molecules occupy three different positions. In each position they are disordered between two orientations with the 0.904/0.096, 0.840/0.160, and 0.532/0.468 occupancies.

DABCO and C₆₀ molecules are statistically disordered between two orientations in **4** and **5**. The type of the C₆₀ disorder is similar to that in **1**. The orientations of DABCO are linked by the rotation of the molecule by 180° about the axis passing through two nitrogen atoms of DABCO. C₆H₅CN and C₆H₄Cl₂ molecules share one position at a 0.7/0.3 ratio in **4**, whereas C₆H₅Cl molecules are disordered between four orientations with the 0.3/0.3/0.2/0.2 occupancies in **5**.

MDABCO⁺ and C₆₀⁻ ions are statistically disordered between two orientations in **6** and **9**. The type of their disorder is similar to that in **4**. C₆H₅CN and C₆H₄Cl₂ molecules share one position at 0.75/0.25 (**6**) and 0.88/0.12 ratios (**9**).

C₆₀⁻ anions are disordered between two orientations in **10** with the 0.551/0.449 occupancies. The orientations are linked by the rotation of C₆₀⁻ anions by 140° about the Co–C(C₆₀⁻) coordination bond. There is one position of the C₆H₄Cl₂ molecules. These molecules are disordered between two orientations with the 0.585/0.415 occupancies.

There are two crystallographically independent C₆₀ molecules in **12**. The position of one C₆₀ is fully occupied. Fullerenes are disordered in this position between four orientations with the 0.35/0.35/0.15/0.15 occupancies. Another position of C₆₀ has only 50% occupancy and lies on the 2-fold symmetry axis of the lattice. Fullerenes in this position and solvent C₆H₄Cl₂ molecules are statistically disordered between two orientations.

Results and Discussion

a. Synthesis of the Complexes. The complexes discussed in this work are listed in Table 1. The M^{II}OEP•C₆₀•(Solvent)_{1.5} complexes (M = Zn, Co, and Fe) were obtained by the diffusion or the evaporation of C₆H₄Cl₂ and C₆H₅Cl solutions containing

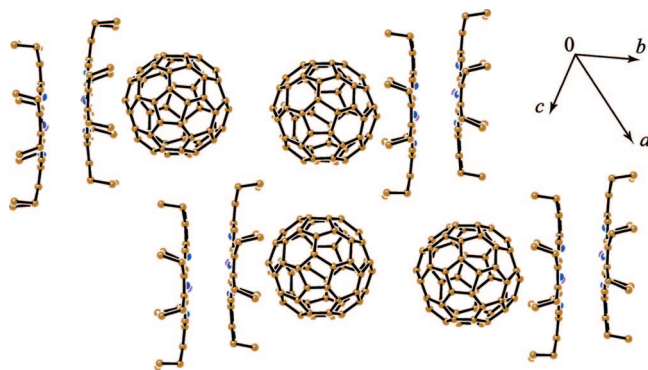


Figure 1. View of the packing of $\text{Fe}^{\text{II}}\text{OEP}$ and C_{60} molecules in **3**. Only major occupied orientation of C_{60} is shown. Solvent molecules are not depicted for clarity.

C_{60} and corresponding porphyrins. These complexes have triclinic unit cells in contrast to previously described complexes with orthorhombic unit cell: $(\text{ZnOEP})_2 \cdot \text{C}_{60} \cdot \text{CHCl}_3$,^{2a} $(\text{ZnOEP})_2 \cdot \text{C}_{60} \cdot (\text{C}_6\text{H}_6)_2$,^{2c} and $(\text{Co}^{\text{II}}\text{OEP})_2 \cdot \text{C}_{60} \cdot \text{CHCl}_3$.^{2a}

DABCO is a bidentate ligand and can form mononuclear or binuclear structures with metalloporphyrins. For example, DABCO forms binuclear structures with metal(II) diethyldithiocarbamates which cocrystallize with C_{60} .¹⁰ Most probably, both mononuclear and binuclear assemblies are formed in the solution containing $\text{M}^{\text{II}}\text{OEP}$ and an excess of DABCO. However, C_{60} cocrystallizes only with mononuclear $\text{M}^{\text{II}}\text{OEP} \cdot \text{DABCO}$ species.

The MDABCO^+ and DMETEP^+ cations coordinate to $\text{M}^{\text{II}}\text{OEP}$ as monodentate ligands to form positively charged $(\text{MDABCO}^+) \cdot \text{M}^{\text{II}}\text{OEP}$ ($\text{M} = \text{Zn}, \text{Co}, \text{Mn}, \text{and Fe}$) and $(\text{DMETEP}^+) \cdot \text{ZnOEP}$ assemblies. The M^{II} atoms are five-coordinated in these assemblies. Since one coordination position at the M^{II} atom is free, $\text{C}_{60}^{\bullet -}$ can also coordinate to $\text{M}^{\text{II}}\text{OEP}$ as in $\{(\text{MDABCO}^+) \cdot \text{Co}^{\text{II}}\text{OEP}\} \cdot (\text{C}_{60}^{\bullet -}) \cdot (\text{C}_6\text{H}_5\text{CN})_{0.67} \cdot (\text{C}_6\text{H}_4\text{Cl}_2)_{0.33}$ (**7**) in which the $\text{Co}-\text{C}(\text{C}_{60}^{\bullet -})$ coordination bonds are formed.^{4g} Coordination assemblies were found in a series of $\{(\text{MDABCO}^+) \cdot \text{M}^{\text{II}}\text{TPP}\} \cdot (\text{C}_{60}^{\bullet -})_2 \cdot (\text{Solvent})_x$ complexes with metal(II) tetraphenylporphyrins ($\text{M} = \text{Zn}, \text{Co}, \text{Mn}, \text{and Fe}$). However, since the MDABCO^+ cations block both coordination positions at the M^{II} atoms, $\text{C}_{60}^{\bullet -}$ cannot approach close to them.^{4d}

A multicomponent ionic complex (**10**) was obtained by diffusion with noncoordinated *N*-methylquinuclidine cations. This complex is formed only with $\text{Co}^{\text{II}}\text{OEP}$, whereas other metal(II) octaethylporphyrins ($\text{M} = \text{Zn}, \text{Fe}^{\text{II}}, \text{and Mn}^{\text{II}}$) do not form such complexes.

b. Crystal Structures. 1. The $\text{M}^{\text{II}}\text{OEP} \cdot \text{C}_{60} \cdot (\text{Solvent})_{1.5}$ Complexes ($\text{M} = \text{Zn}, \text{Co}, \text{and Fe}$, **1–3).** Fullerene molecules are ordered in **2** and they are disordered between two orientations in **1** and **3**. Complexes with ZnOEP and $\text{Co}^{\text{II}}\text{OEP}$ are isostructural, whereas **3** has two crystallographically independent C_{60} and $\text{Fe}^{\text{II}}\text{OEP}$ molecules and greater parameter *a*. **1–3** have similar structural motifs: the pairs of the C_{60} molecules alternate with those of the $\text{M}^{\text{II}}\text{OEP}$ ones (Figure 1). The center-to-center distances of 9.998 (**1**), 9.921 (**2**), and 10.191 Å (**3**) between C_{60} in the pairs allow the formation of $\text{C} \cdots \text{C}$ contacts shorter than the sum of van der Waals radii of two carbon atoms (3.45 Å).¹¹ Porphyrin fragments are shifted in the $\text{M}^{\text{II}}\text{OEP}$ pairs in such a way that the M^{II} atom of one porphyrin molecule is located below the nitrogen atom of the neighboring porphyrin. As a result, metal–metal distances are rather short in **1–3** (3.148–3.448 Å, Table 3) and all eight ethyl substituents of $\text{M}^{\text{II}}\text{OEP}$ are oriented in one direction toward fullerene (Figures

1 and **2**). Similar structural motifs were found in the C_{70} complexes with $\text{M}^{\text{II}}\text{OEP}$ ($\text{M} = \text{Zn}, \text{Co}, \text{and Cu}$)^{2a} and in the C_{60} complexes with $\text{M}^{\text{II}}\text{OEP}$ ($\text{M} = \text{Ni}, \text{Pt}, \text{Pd}, \text{Ag}, \text{and Cu}$).^{2c,12} For the latter complexes porphyrin molecules are more strongly shifted relative to each other in the $\text{M}^{\text{II}}\text{OEP}$ pairs that provides longer $\text{M} \cdots \text{M}$ distances (4.47–4.68 Å, Table 3) and only four of eight ethyl substituents of $\text{M}^{\text{II}}\text{OEP}$ are oriented toward fullerene.

Coordination between ZnOEP and C_{60} is absent in **1** since the shortest $\text{Zn} \cdots \text{C}(\text{C}_{60})$ distances are 2.885 and 2.995 Å for two orientations of C_{60} . The shorter $\text{Co} \cdots \text{C}(\text{C}_{60})$ distance of 2.685 Å in **2** indicates weak bonding between $\text{Co}^{\text{II}}\text{OEP}$ and C_{60} . The $\text{Fe} \cdots \text{C}(\text{C}_{60})$ distance of 2.622 Å for one of two crystallographically independent C_{60} molecules in **3** (Figure 2) is the shortest one among those for the neutral $\text{M}^{\text{II}}\text{OEP}-\text{C}_{60}$ complexes. The Fe^{II} atom involved in this contact displaces by 0.002 Å out of the plane of four nitrogen atoms toward C_{60} . Close lengths of the $\text{M} \cdots \text{C}(\text{C}_{60})$ contacts were found in molecular C_{60} complexes with metal tetraarylporphyrins: 2.58–2.63 Å for $\text{Fe}^{\text{II}}\text{TPP}$,^{13a} 2.57 Å for $\text{Fe}^{\text{III}}\text{TPP}^+$,^{13b} and 2.58–2.69 Å for cobalt(II) tetraarylporphyrins.^{13c,4e} Metal(II) octaethylporphyrins, which have no tendency to extra coordination ($\text{M} = \text{Ni}, \text{Pt}, \text{Pd}, \text{Ag}, \text{and Cu}$), form longer $\text{M} \cdots \text{C}(\text{C}_{60})$ contacts (3.002–3.098 Å) in the complexes with C_{60} (Table 3).^{2c,12}

Porphyrin macrocycles are planar in **1–3** (the rms deviations are from 0.059 to 0.097 Å). For the M^{II} atoms in **1**, **2** and one crystallographically independent $\text{Fe}^{\text{II}}\text{OEP}$ in **3** (with longer $\text{Fe} \cdots \text{C}(\text{C}_{60})$ distance of 2.647 Å), a small out-of-plane displacement from the plane of four nitrogen atoms toward neighboring $\text{M}^{\text{II}}\text{OEP}$ is observed (Table 3). This displacement can be due to weak coordination of the metal(II) centers to the nitrogen atoms of neighboring porphyrin molecules.

b. Isostructural Complexes 4–11. Molecular $\{\text{M}^{\text{II}}\text{OEP} \cdot \text{DABCO}\} \cdot \text{C}_{60} \cdot (\text{Solvent})_x$ ($\text{M} = \text{Zn}$ and Co), ionic $\{(\text{MDABCO}^+) \cdot \text{M}^{\text{II}}\text{OEP}\} \cdot (\text{C}_{60}^{\bullet -}) \cdot (\text{Solvent})_x$ ($\text{M} = \text{Zn}, \text{Co}, \text{and Mn}$) and $(\text{MQ}^+) \cdot \{\text{Co}^{\text{II}}\text{OEP} \cdot (\text{C}_{60}^{\bullet -})\} \cdot \text{C}_6\text{H}_4\text{Cl}_2$ complexes as well as previously described complexes **7** and **11** are isostructural (Table 2) and will be discussed together.

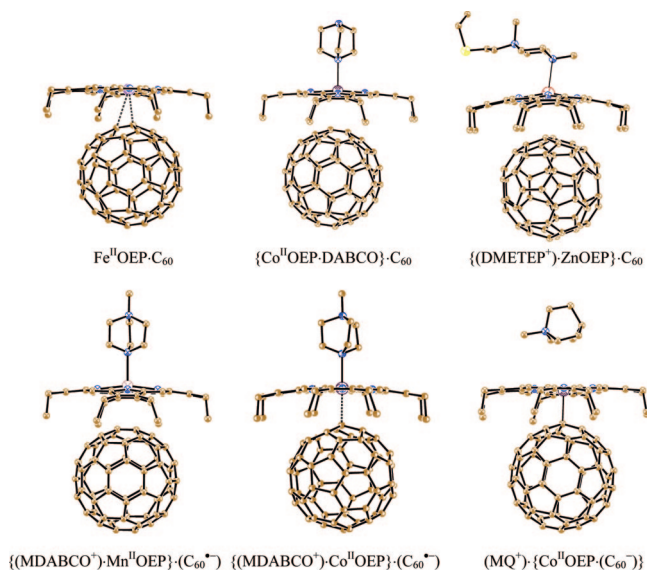
The main structural motif of these complexes is zigzag chains of fullerenes, which occupy channels formed by four $\text{M}^{\text{II}}\text{OEP}$ molecules (Figure 3a). Due to a zigzag arrangement of fullerenes in the chains vacancies are formed (Figure 3b), which accommodate small ligands and cations (DABCO , MDABCO^+ , MQ^+ , and TMP^+). There are also vacancies in the walls of the channels occupied by disordered solvent molecules at different ratio (Figure 3a). The center-to-center distances between fullerenes in the chains are defined by the size of ligands and cations. The shortest distances were found in the complexes with MQ^+ (9.884 Å, **10**), DABCO (9.968 Å, **4** and 9.936 Å, **5**) and TMP^+ (10.026 Å, **11**)^{4g}. In this case from two to five van der Waals $\text{C} \cdots \text{C}$ contacts are formed between fullerenes in the 3.160–3.395 Å range. The longer center-to-center distances were found in the complexes with the MDABCO^+ cations (10.297 Å for **7**,^{4g} 10.560 Å for **6** and 10.703 Å for **9**), which prevent the formation of van der Waals $\text{C} \cdots \text{C}$ contacts between $\text{C}_{60}^{\bullet -}$.

C_{60} and $\text{C}_{60}^{\bullet -}$ are disordered in **4–7** and **9–12**. The character of disorder is similar in **4–6**, and **9**. There are two orientations with approximately 0.50/0.50 occupancies, which are linked by the rotation of the fullerene molecules (anions) by 180° about a 3-fold axis passing through the centers of two oppositely located hexagons. The disorder is retained even in the presence of the $\text{Co}-\text{C}(\text{C}_{60}^{\bullet -})$ coordination bonds in ionic **7**, **10**, and **11**. In this case $\text{C}_{60}^{\bullet -}$ anions rotate by 140° about this bond.

Table 3. Lengths of the M \cdots C(C₆₀ or C₆₀⁻), the M \cdots M Contacts, the M–N(L) and Averaged M–N(OEP) Bonds in the Complexes of C₆₀ with Metal(II) Octaethylporphyrins

M	M ^{II} OEP·C ₆₀ , Å	(M ^{II} OEP·DABCO)·C ₆₀ , Å	(C ⁺)·{M ^{II} OEP·(C ₆₀ ⁻)}, Å with noncoordinating cations	(C ⁺)·M ^{II} OEP·(C ₆₀ ⁻), Å with coordinating cations
Fe	2.622, 2.622 ^d (Comp. 3) 2.647, 2.662 ^d (Fe \cdots C) ^a 3.418, 3.448 (Fe \cdots Fe) ^a 1.977(2), 1.981(2) (Fe–N(OEP)) ^a –0.002 (0.081)/0.059 ^{b,c} 0.017 (0.101)/0.068 ^{a,b}		complex was not formed	crystal structure was not solved (Comp. 8)
Co	(Comp. 2) 2.685, 2.841 (Co \cdots C) 3.400 (Co \cdots Co) 1.977(1) (Co–N(OEP)) 0.025 (0.118)/0.071 ^b	2.844, 3.129 (Comp. 5) 2.957, 3.030 (Co \cdots C) ^d 2.291(6), 2.347(6) (Co–N(L)) ^f 1.996(3) (Co–N(OEP)) 0.153 (0.296)/ 0.154 ^b	C ⁺ = MQ ⁺ (Comp. 10) 2.266(3) (Co–C), 1.984(3) (Co–N(OEP)), –0.115 (–0.055)/ 0.061 ^{b,c} C ⁺ = TMP ⁺ (Comp. 11) ^{4g} 2.268(1) (Co–C), 1.978(2) (Co–N(OEP))	C ⁺ = MDABCO ⁺ (Comp. 7) ^{4g} 2.508(4) (Co–C) 2.340(3) (Co–N(L)) 1.983(5) (Co–N(OEP))
Zn	2.885 (Comp. 1) 2.995, 3.133 (Zn \cdots C) ^d 3.148 (Zn \cdots Zn) 2.055(1) (Zn–N(OEP)) 0.200 (0.336)/0.097 ^b	3.153, 3.183 (Comp. 4) 3.260, 3.322 (Zn \cdots C) ^d 2.182(2) (Zn–N(L)) 2.090(3) (Zn–N(OEP)) 0.387 (0.596)/0.154 ^b	complex was not formed	C ⁺ = MDABCO ⁺ (Comp. 6) 3.063, 3.123 3.037, 3.069 (Zn \cdots C) ^d 2.237(2) (Zn–N(L)) 2.065(4) (Zn–N(OEP)) 0.239 (0.413)/ 0.145 ^b C ⁺ = DMETEP ⁺ (Comp. 12) 3.172 (Zn \cdots C) ^d 2.396(2) (Zn–N(L)) 2.071(3) (Zn–N(OEP)) 0.307 (0.514)/ 0.162 ^b
Mn			complex was not formed	C ⁺ = MDABCO ⁺ (Comp. 9) 3.049, 3.124 3.096, 3.133 (Mn \cdots C) ^d 2.301(1) (Mn–N(L)) 2.107(2) (Mn–N(OEP)) 0.274 (0.470)/ 0.152 ^b
Ni	3.002, 3.204 (Ni \cdots C) 4.678 (Ni \cdots Ni) ^{12a}			
Cu	3.024, 3.212 (Cu \cdots C) 4.561 (Cu \cdots Cu) ^{2c}			
Pd	3.084, 3.181 (Pd \cdots C) 4.599 (Pd \cdots Pd) ^{2c}			
Pt	3.084, 3.237 (Pt \cdots C) 4.633 (Pt \cdots Pt) ^{12b}			
Ag	3.098, 3.239 (Ag \cdots C) 4.476 (Ag \cdots Ag) ^{2c}			

^a For two crystallographically independent C₆₀ and Fe^{II}OEP molecules. ^b Deviation of metal atoms from the mean plane of four nitrogen atoms (deviation of metal (II) atoms from the mean 24-atom porphyrin plane)/root-mean square (rms) deviations of metal atoms from the mean 24-atom porphyrin plane. All values are given in Å. ^c Negative value corresponds to the deviation of metal atoms toward fullerene, positive value toward DABCO or MDABCO⁺. ^d For both orientations of C₆₀ or C₆₀⁻. ^e For major occupied orientation of C₆₀. ^f For two orientations of DABCO.

**Figure 2.** Different coordination modes of the ligands and fullerenes to M^{II}OEP. Only major occupied orientation is depicted for disordered C₆₀⁻, C₆₀, DABCO, and MDABCO⁺.

Obviously, electrostatic interaction between the closely packed cations and C₆₀⁻ cannot fix fullerene disorder.

Both neutral DABCO and the MDABCO⁺ cations form coordination assemblies with M^{II}OEP that allow one to study the effect of positive charge on coordination ability of these ligands. The length of the M–N(L) bonds are 2.182(2) (**4**) and 2.291(6) Å (**5**) for neutral DABCO, and 2.237(2) (**6**) and 2.340(3) Å (**7**) for the MDABCO⁺ cation. Therefore, the 0.049–0.055 Å elongation of the bonds is observed for the cation. Previously, the effect of negative charge of ligand on the M–N(L) bonds length was found. Neutral 2-MeIm and the 2-MeIm⁻ anion form the Fe–N(L) bonds of different lengths with Fe^{II}OEP: 2.147 and 2.058 Å. The 2-MeIm⁻ anion is a stronger field ligand and better σ -donor than 2-MeIm and that can explain the shortening of the Fe–N(2-MeIm⁻) bonds by ~0.09 Å.¹⁴ In our case positive charge of MDABCO⁺ decreases its σ -donor properties and elongates the M–N(L) bonds. The M–N(L) bonds (2.301(1)–2.340(3) Å) are noticeably shorter for (MDABCO⁺)·M^{II}OEP than for (MDABCO⁺)₂·M^{II}TPP (M = Co^{II} and Mn^{II}) - 2.475(2) and 2.511(3)–2.553(2) Å, respectively.^{4d}

C₆₀ or C₆₀⁻ are arranged from the opposite side of the porphyrin macrocycle relative to the N-containing ligand. The

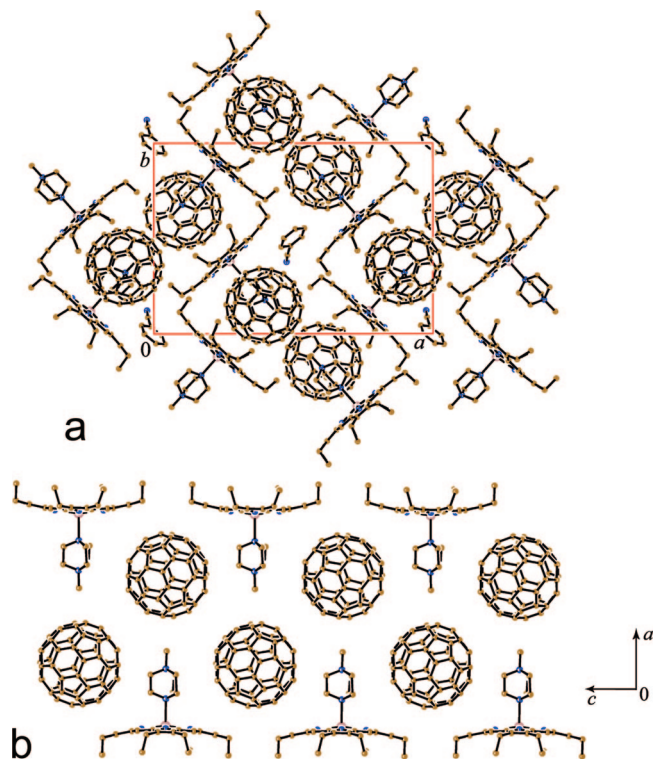


Figure 3. View of the crystal structure of **9** along the *c*- (a) and *b*-axes (b). One orientation is depicted for the disordered $C_{60}^{\bullet-}$ and MDABCO $^+$. Only C_6H_5CN solvent molecules are shown in one of two orientations.

$M^{\bullet\bullet} \cdots C(C_{60})$ distances are equal to 3.175 Å (ZnOEP) and 2.829 Å (Co $^{\text{II}}$ OEP, Figure 2) in **4** and **5**, respectively. Therefore, the coordination of DABCO increases the $M^{\bullet\bullet} \cdots C(C_{60})$ distances as compared with those distances for DABCO free complexes **1** and **2**. The reason for that is the displacement of the M^{II} atoms from the plane of four nitrogen atoms toward DABCO by 0.387 Å in **4** and 0.153 Å in **5**. Among ionic complexes the shortest $Co^{\bullet\bullet} \cdots C(C_{60}^{\bullet-})$ distance was previously found in **7** (2.508(4) Å at 100 K, Figure 2) and in this case real coordination Co–C bond is formed since both spins from Co $^{\text{II}}$ OEP and $C_{60}^{\bullet-}$ are paired at its formation.^{4g} The $M^{\bullet\bullet} \cdots C(C_{60}^{\bullet-})$ distances in **6** and **9** are essentially longer (Figure 2) (3.037 and 3.049 Å at 100 K, respectively) indicating the absence of coordination of $C_{60}^{\bullet-}$ to ZnOEP or Mn $^{\text{II}}$ OEP. The M^{II} atoms deviate from the plane of four nitrogen atoms toward MDABCO $^+$ by 0.042 Å in **7**,^{4g} 0.239 Å in **6** and 0.274 Å in **9**. The $C_{60}^{\bullet-}$ radical anions form multiple short van der Waals $N^{\bullet\bullet} \cdots C$ and $C^{\bullet\bullet} \cdots C$ contacts with the porphyrin macrocycles in **6**, **7**, and **9** since these macrocycles are concave-shaped and conform well to the spherical shape of C_{60} (Figure 2).

The MQ^+ cation is not coordinated to Co $^{\text{II}}$ OEP in **10** to provide the formation of stable Co–C($C_{60}^{\bullet-}$) σ -bonds (Figure 2). The bond length of 2.266(3) Å is close to the length of the Co–C($C_{60}^{\bullet-}$) bonds in **11** - 2.268(1) Å^{4g} and in ionic multi-component complexes with Co $^{\text{II}}$ TPP - 2.28–2.32 Å.^{4e} The Co $^{\text{II}}$ atoms deviate by 0.115 Å from the plane of four nitrogen atoms toward $C_{60}^{\bullet-}$.

c. Crystal Structure of Complex 12. Complex **12** contains the DMETEP $^+$ cation which has a long $-CH_2-CH_2-S-CH_2-CH_3$ substituent. As a result, the crystal structure of **12** is different from those of other complexes studied. Moreover, there are two crystallographically independent C_{60} molecules in **12**. The molecules of one type locate in zigzag chains alternating

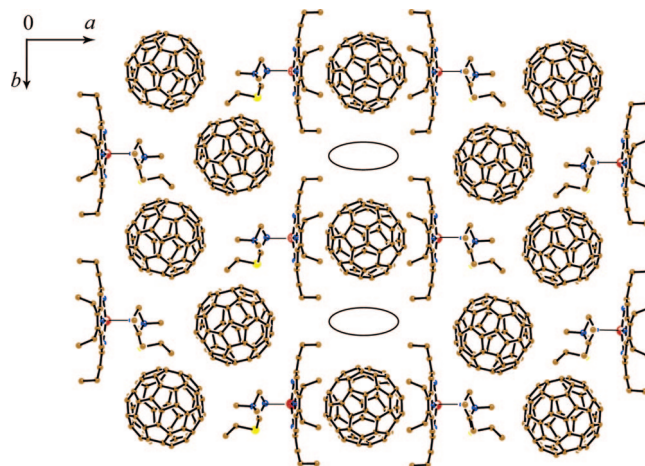


Figure 4. The fragment of the crystal structure of **12** viewed along the *c*-axis. Only one orientation for disordered fullerene molecules is shown. Solvent $C_6H_4Cl_2$ molecules are omitted for clarity.

with the DMETEP $^+$ cations with a center-to-center interfullerene distance of 10.074 Å. The molecules of the other type locate in vacancies formed by 16 ethyl substituents of two ZnOEP molecules (Figure 4). The composition of **12** indicates that there is only one DMETEP $^+$ cation per 1.5 C_{60} molecules. Therefore, in this complex two fullerene molecules in neutral and anionic state or fullerene spheres are partially charged. Unfortunately, the disorder of fullerenes does not allow one to distinguish between these two cases. However, that can be made by optical methods.

The vacancies between fullerenes in the zigzag chains cannot accommodate long $-CH_2-CH_2-S-CH_2-CH_3$ substituents of the cations. As a result, the channels from porphyrin molecules characteristic of complexes **4–11** do not form in **12**. Instead of that layers consisting of the (DMETEP $^+$)· C_{60} and (ZnOEP) $_2$ · C_{60} chains alternating along the *a*-axis are formed (Figure 4). The layers are arranged in such a way that the (ZnOEP) $_2$ · C_{60} chains locate above and below the (DMETEP $^+$)· C_{60} chains from the neighboring layers. Large vacancies in the (ZnOEP) $_2$ · C_{60} chains (shown by ovals in Figure 4) are occupied by solvent $C_6H_4Cl_2$ molecules and long substituents of the DMETEP $^+$ cations from the neighboring layers.

The length of the Zn–N(DMETEP $^+$) bonds in the (DMETEP $^+$)·ZnOEP coordination units of 2.396(2) Å (Figure 2) is essentially longer than the length of such bonds in the coordination units of ZnOEP with DABCO and the MDABCO $^+$ cations (2.182(2)–2.237(2) Å).

c. Optical Properties. Detailed IR- and UV–visible–NIR spectra of the complexes are given in Supporting Information. The bands of the $F_{1u}(4)$ mode, which is most sensitive to charge transfer to the C_{60} molecules,¹⁵ are at 1424–1429 cm^{-1} in the spectra of **3** and **4** and at 1387–1399 cm^{-1} in the spectra of **6–10**. Therefore, **3** and **4** are molecular complexes and **6–10** are ionic ones. The UV–visible–NIR spectra of the complexes are presented in Figure 5 and the positions of the bands are listed in Table 4. Complex **4** shows a weak broad band at 760 nm (Figure 5b). This band can be attributed to charge transfer (CT) from ZnOEP·DABCO units to C_{60} . Similar bands were found in the C_{60} complexes with coordination (ZnTPP) $_x$ ·L ($x = 1, 2$ and 4)¹⁶ and (ZnOEP) $_2$ ·BPY assemblies.^{4a} The appearance of the bands characteristic of $C_{60}^{\bullet-}$ at 933–938 and 1075–1078 nm^{1b,6a} in the spectra of **6–9** (Figure 5c, Table 4) indicates their ionic ground state. The spectrum of **10** is different from those of **6–9** because a new intense band appears at 1270

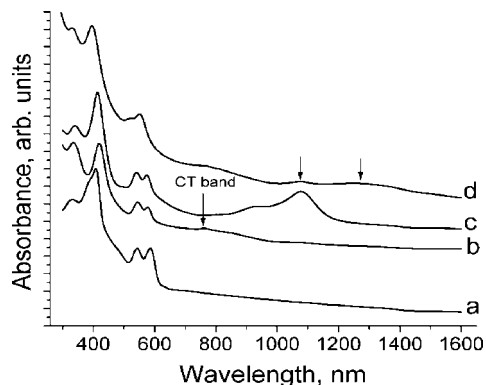


Figure 5. The spectra of starting ZnOEP (a); **4** (b); **6** (c); and **10** (d) in KBr pellets at RT.

Table 4. UV-vis-NIR Spectra of Starting Compounds and the Obtained Complexes

compound	porphyrin		fullerene		charge transfer bands, nm
	Soret band, nm	Q-bands, nm	UV, nm	NIR, nm	
C ₆₀			341		
ZnOEP	409	542, 586			
Co ^{II} OEP	394	531, 560			
Fe ^{II} OEP	383	546, 573			
Mn ^{II} OEP	420	554, 589			
4 (ZnOEP)	419 (10)	545, 577	335		760
6 (ZnOEP)	414 (5)	540, 574	340	936, 1075	
12 (ZnOEP)	414 (5)	540, 574	340	937, 1074	
7 (Co ^{II} OEP)	402 (6)	522, 549	333	933, 1078	4g
10 (Co ^{II} OEP)	396 (2)	523, 550	331	1076, 1270	
11 (Co ^{II} OEP)	398 (4)	523, 552	330	1086, 1277	4g
3 (Fe ^{II} OEP)	383 (0)	—, 560	333		
8 (Fe ^{II} OEP)	409 (26)	535, 552	340	938, 1076	
9 (Mn ^{II} OEP)	426 (6)	550, 582	342	935, 1077	

nm additionally to the band at 1076 nm (intramolecular transitions in the C₆₀⁻ anions) (Figure 5d). The latter band can be ascribed to CT between closely packed Co^{II}OEP and C₆₀⁻ in the σ -bonded {Co^{II}OEP·(C₆₀⁻)} units. This band was previously observed in other complexes containing the σ -bonded {Co^{II}porphyrin·(C₆₀⁻)} units.^{4c,g} The absence of such CT bands in the spectra of **6–9** allows one to suppose that the coordination M–C(C₆₀⁻) bonds do not form in these complexes at RT.

The Soret and Q-bands of M^{II}OEP are very sensitive to the coordination of ligands. In this case the red shift of the Soret band is observed (Table 4). The greatest shift of 26 nm was found at the formation of (MDABCO⁺)·Fe^{II}OEP. It is interesting that in spite of rather short Fe···C(C₆₀) contacts in **3**, there is no shift of the Soret band in its spectrum. The data show that the coordination of the N-containing ligands to M^{II}OEP essentially more strongly shifts the Soret band to the red side than weak coordination of C₆₀ or C₆₀⁻ (Table 4).

There is only one DMETEP⁺ cation per 1.5 fullerene molecules in **12**. The IR-spectrum of **12** shows the bands of F_{1g}(4) mode at two positions: the split band at 1388, 1390, and 1394 cm⁻¹ and the band at 1430 cm⁻¹. The position of the former band indicates the formation of C₆₀⁻ (this band was found in the spectra of C₆₀⁻ complexes at 1388–1396 cm⁻¹).^{1b,6a,15} The position of the latter band indicates the presence of neutral C₆₀.¹⁵ Therefore, neutral and -1 charged fullerene species can be distinguished from the IR spectra. Partial charge transfer is most probably not realized in **12** since in this case the bands with intermediate position between those characteristic of neutral and -1 charged C₆₀ should be observed. UV-visible-NIR spectrum of **12** contains bands characteristic

of C₆₀⁻ at 937 and 1074 nm. The bands at 262 and 340 nm in the UV range can be attributed to both neutral and -1 charged C₆₀.

d. Magnetic Properties of the Complexes. Optical data indicate that **3** is a molecular complex without charge transfer from Fe^{II}OEP to C₆₀. EPR measurements support this conclusion since no EPR signals are observed in the spectrum of **3** from RT down to 4 K. That is consistent with the presence of EPR silent neutral C₆₀ and Fe^{II}OEP with odd spin state. Effective magnetic moment of **3** is equal to 2.76 μ_B at 300 K. This value corresponds to the intermediate ($S = 1$) spin state of Fe^{II}OEP (the calculated value for the system containing one uncoupled $S = 1$ spin is 2.83 μ_B). It is known that the spin state of Fe^{II}porphyrins affects the length of the Fe–N(porphyrin) bonds. They are short in low-spin Fe^{II}TPP·(Pip)₂ (2.004(3) Å, Pip is piperidine)^{17a} and elongate in the high-spin ($S = 2$) five- and six-coordinated Fe^{II}porphyrin·L(L₂) units to 2.057(4)–2.118(13) Å (ref 17b and references therein). The averaged length of the Fe–N(OEP) bonds of 1.977(2)–1.981(2) Å in **3** corresponds to the low or intermediate spin state of Fe^{II}OEPa in accordance with magnetic measurements. Fe^{II}TPP has also intermediate spin state in the complex with C₆₀ ($S = 1$).^{13a} Complex **3** manifests a positive Weiss temperature of 2.6 K in the 50–300 K range (Figure 6d) indicating weak ferromagnetic interaction of spins. This interaction can be realized within the Fe^{II}OEP pairs with a rather short Fe···Fe distance of 3.418 and 3.448 Å (for two crystallographically independent Fe^{II}OEP). In molecular Ag^{II}OEP·C₆₀·(C₆H₆)₂ complex with a longer Ag···Ag distance of 4.476 Å, a weaker antiferromagnetic (AF) interaction of spins is observed (the Weiss temperature is -0.7 K).¹⁸

Complex **6** contains paramagnetic C₆₀⁻ and diamagnetic ZnOEP. Magnetic moment of **6** ($\mu_{\text{eff}} = 1.60 \mu_B$ at 300 K) corresponds to the contribution of about one 1/2 spin per formula unit, which is localized on C₆₀⁻ ($S = 1/2$). The Weiss temperature is negative ($\Theta = -17.8$ K, Figure 6c) indicating AF interaction of spins. Since C₆₀⁻ radical anions are arranged in zigzag chains in **6**, it can be supposed that magnetic interaction is realized namely within these chains. Interchain interaction is weak because of large distances between the chains. Previously described {(MDABCO⁺)₂·M^{II}TPP}·(C₆₀⁻)₂·(Solvent)_x complexes (M = Zn, Mn, and Fe) also contain chains formed by C₆₀⁻ and demonstrate AF interaction of spins with the Weiss temperatures from -2 to -13 K.^{4d} Complex **6** manifests a single Lorenz line with $g = 1.9990$ and the line width (ΔH) of 2.43 mT at RT (Figure 7a) attributed to C₆₀⁻ (generally C₆₀⁻ manifest signal with $g = 1.996–2.000$ and $\Delta H = 2–6$ mT at RT).^{1b,19} The signal narrows with the temperature decrease (Figure 7d). Below 120 K it splits into two components (Figure 7b) whose g -factors are shifted in the opposite directions with the temperature decrease and the components are slightly broadened at low temperatures (Figure 7c,d). The deviation of reciprocal molar susceptibility from the Curie–Weiss law below 20 K (Figure 6c) indicates weak ferromagnetic interaction of spins.

Complex **12** shows very similar magnetic behavior (Table 5) with the splitting of the EPR signal into two components below 120 K.

Magnetic moment of **8** is equal to 4.85 μ_B at 300 K. The value calculated for the system of two uncoupled ($S = 2 + 1/2$) spins is 5.19 μ_B . Therefore, the (MDABCO⁺)·Fe^{II}OEP units can be in a high spin state ($S = 2$) as was previously observed for other five-coordinated Fe^{II}OEP·L porphyrins.¹⁷ However, the justification of the spin state of Fe^{II}OEP from structural data is needed. The complex manifests a strongly negative Weiss

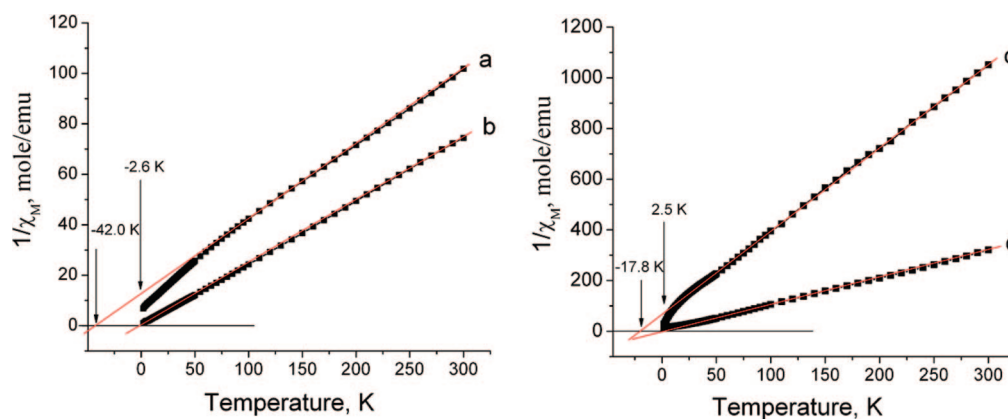


Figure 6. Temperature dependences of reciprocal molar magnetic susceptibility fitted by the Curie–Weiss expression $\chi \propto (T - \Theta)^{-1}$ within the Θ values listed in Table 5: (a) **9**; (b) **8**; (c) **6**; and **3** (d).

Table 5. Data of Magnetic and EPR Measurements

complex	EPR			SQUID		
	<i>g</i> -factor	ΔH , mT (T, K)	attribution	μ_{eff} , μ_B	calculated μ_{eff} , μ_B (per formula unit)	Θ , K (range)
3	ESR signal is absent			2.76	2.83 ($S = 1$, Fe ^{II} OEP)	2.56 (50–300 K)
6	1.9990	2.43 (RT)	$C_{60}^{\bullet-}$	1.60	1.73 ($S = 1/2$, $C_{60}^{\bullet-}$)	-17.8 (50–300 K)
12	1.9965	0.62	split signal, $C_{60}^{\bullet-}$	4.85	5.19 ($S = 2 + 1/2$, Fe ^{II} OEP and $C_{60}^{\bullet-}$)	-42 (100–300 K)
	2.0002	0.37 (4 K)				
8	1.9990	3.84 (RT)	split signal, $C_{60}^{\bullet-}$ (Fe ^{II} OEP + $C_{60}^{\bullet-}$)	4.85	5.19 ($S = 2 + 1/2$, Fe ^{II} OEP and $C_{60}^{\bullet-}$)	-42 (100–300 K)
	1.9965	0.49				
9	2.4230	268	weak, $C_{60}^{\bullet-}$	5.48	6.16 ($S = 5/2 + 1/2$, Mn ^{II} OEP and $C_{60}^{\bullet-}$)	-2.46 (10–300 K)
	1.9992	3.4 (RT)				
At low temperatures signal cannot be observed due to the large line width						
10	5.46	60	Mn ^{II} OEP	5.48	6.16 ($S = 5/2 + 1/2$, Mn ^{II} OEP and $C_{60}^{\bullet-}$)	-2.46 (10–300 K)
	2.3418	40	(Mn ^{II} OEP + $C_{60}^{\bullet-}$)			
10	1.9944	3.26 (RT)	$C_{60}^{\bullet-}$	Diamagnetic. Curie tail corresponds to the contribution of about 5% of spins from total amount of Co ^{II} OEP and $C_{60}^{\bullet-}$		
	2.5442	94.8	Co ^{II} OEP			
	1.9998	4.0	$C_{60}^{\bullet-}$			
	2.0011	0.36 (RT)	impurity ($C_{120}O$)			

temperature of -42 K, but the spin ordering is not observed in **8** down to 1.9 K (Figure 6a). The deviation of reciprocal molar susceptibility from the Curie–Weiss law below 60 K indicates that the coupling of spins at low temperatures has ferromagnetic nature (Figure 6a).

A very broad EPR signal of **8** with *g*-factor of 2.4230 and ΔH of 268 mT at RT (Figure 8a) was ascribed to both

paramagnetic Fe^{II}OEP and $C_{60}^{\bullet-}$ species having strong exchange coupling. This interaction results in the appearance of one Lorenz signal instead of two signals from individual Fe^{II}OEP and $C_{60}^{\bullet-}$. The signal is even more broadened with the temperature decrease and cannot be observed at low temperatures. There is also a weak signal with *g* = 1.9992 (ΔH = 3.4 mT) at RT (Figure 8a). It is rather broad at RT and strongly

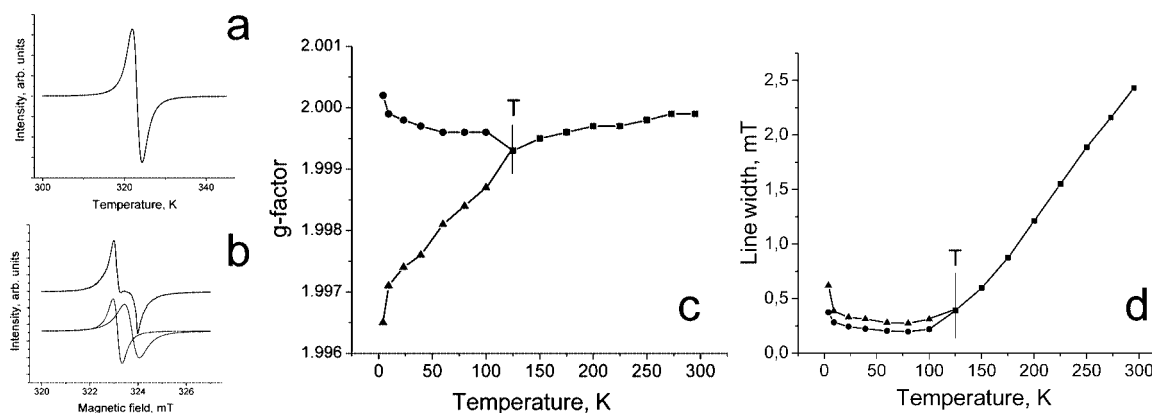


Figure 7. The EPR signal in **6** at RT (a) and at 4 K (b). In panel b below the observed EPR signal is shown the fitting of the signal by two Lorentz lines. Temperature dependence of *g*-factor (c) and the line width (d) of the signal.

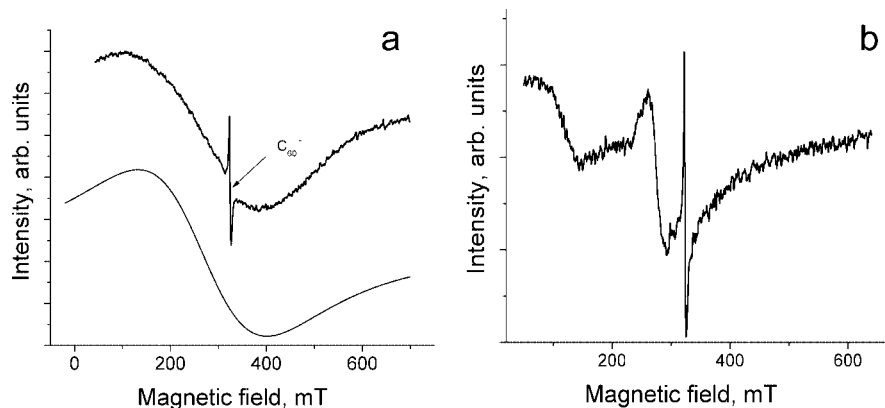


Figure 8. EPR signals: (a) of polycrystalline **8** at RT. Below the fitting of the signal by Lorenz line is shown; (b) of polycrystalline **9** at RT.

narrows with the temperature decrease allowing to attribute this signal to C₆₀^{•-}.^{1b,19} The intensity of the signal is several orders of magnitude lower than that of the broad signal.

Magnetic moment of **9** is equal to 5.48 μ_B at 300 K. The calculated value for the system with two uncoupled ($S = 5/2 + 1/2$) spins is 6.16 μ_B . Therefore, high-spin state ($S = 5/2$) of Mn^{II}OEP is suggested. The length of the Mn–N(OEP) bonds in **9** of 2.107(2) Å also proves the high-spin state of Mn^{II}OEP. Close length of the Mn–N(porphyrin) bonds was found in the high-spin Mn^{II}TPP•(1-MeIm) (2.128(7) Å^{20a}) and (MDABCO⁺)₂•Mn^{II}TPP (2.096–2.097(2) Å).^{4d} Manganese(II) octaethyl- and tetraphenylporphyrates generally have a high $S = 5/2$ spin state^{20b} and only at the coordination of NO the lowering of the spin state of Mn^{II}TPP was found.^{20c} Complex **9** manifests small Weiss temperature of –2.5 K indicating only weak AF interaction of spins. The reason for that is a large distance between C₆₀^{•-} in the chains and a rather large distance between the Mn^{II} atoms and the C₆₀^{•-} carbon atoms (larger than those in **6** and **7**). A complicate EPR spectrum of **9** consists of three signals (Figure 8b, Table 5). The signal with $g > 5$ according to g -factor value can be ascribed to high-spin Mn^{II}OEP,^{20b} a broad weak signal with $g = 1.9944$ ($\Delta H = 3.26$ mT) was ascribed to C₆₀^{•-}, and an intense signal with $g = 2.3418$ ($\Delta H = 40$ mT) was attributed to both paramagnetic Mn^{II}OEP and C₆₀^{•-} species having strong exchange coupling. This signal has a g -factor value intermediate between those characteristic of Mn^{II}OEP and C₆₀^{•-}. Previously studied {(MDABCO⁺)₂•Mn^{II}TPP}•(C₆₀^{•-})₂•(Solvent)_x complex manifests a similar asymmetric signal with a g -factor close to 2.4 at RT.^{4d}

Complex **10** is a diamagnetic one due to the formation of the Co–C(C₆₀⁻) bonds. The Curie tail corresponds to the contribution of only 5% of spins from a total amount of Co^{II}OEP and C₆₀^{•-}. The RT EPR spectrum of **10** shows that this contribution is provided by spins localized on Co^{II}OEP ($g = 2.5442$ and $\Delta H = 94.8$ mT) and C₆₀^{•-} ($g = 1.9998$ and $\Delta H = 4$ mT) retained in the sample due to the presence of defects. Weak EPR signals were previously observed in **11** having similar Co–C bonds but the estimated amount of impurities was only 2% from a total amount of Co^{II}OEP and C₆₀^{•-}.^{4g} The dissociation of the Co–C(C₆₀⁻) bonds in **7** is accompanied by the appearance of a new EPR signal with $g = 2.1188$ and $\Delta H = 52$ mT (RT).^{4g} Since such signal is not observed in **10** up to RT, we can conclude that the σ -bonded {Co^{II}OEP•(C₆₀⁻)} anions are stable in this complex up to RT.

Conclusion

New molecular C₆₀ complexes with ZnOEP, Co^{II}OEP, and Fe^{II}OEP crystallize in C₆H₄Cl₂ and C₆H₅Cl as triclinic phases

(**1–3**). Since solvent molecules are involved in the complexes their size affects the crystal packing. Solvent molecules with a small size (CHCl₃, C₆H₆) provide the formation of orthorhombic phases,^{2a,c,12} whereas triclinic phases are formed in solvents with a larger size of the molecules.

It is known that the HOMO–LUMO overlapping of donor and acceptor defines the intensity of CT bands in the spectrum of the complex and affects the degree of charge transfer from donor to acceptor.²¹ No CT bands are observed in the spectra of the C₆₀ complexes with planar metal(II) octaethylporphyrins (as in **3**). Similarly, CT bands are either absent or very weak in the spectra of fullerene complexes with metal(II) tetraphenylporphyrins.^{2c} The reason for that can be an ineffective HOMO–LUMO overlapping between nearly spherical C₆₀ molecules and planar porphyrin planes. Probably namely ineffective HOMO–LUMO overlapping hinders CT in the ground-state of **3** from relatively strong donor Fe^{II}OEP²² to C₆₀ and defines the neutral ground-state of the complex. Coordination of the ligand to M^{II}OEP provides a concave shape of the porphyrin macrocycles, M^{II}OEP•L, which better corresponds to the C₆₀ sphere. As a result, complex **4** containing the DABCO•ZnOEP coordination units manifests a CT band in the visible–NIR spectrum.

The tendency of metalloporphyrins to extra coordination can successfully be used in the design of molecular and ionic complexes of M^{II}OEP with neutral and negatively charged fullerenes. Molecular {M^{II}OEP•DABCO}•C₆₀•(Solvent)_x complexes crystallize in the presence of the DABCO ligand, whereas the coordinating MDABCO⁺ and DMETEP⁺ cations can cocrystallize with C₆₀^{•-} in the presence of porphyrin to form ionic {(L⁺)•M^{II}OEP}•(C₆₀^{•-})•(Solvent)_x complexes. The driving force for the formation of these complexes is the coordination of the N-containing ligands and cations to M^{II}OEP (M = Zn, Co, Mn, and Fe). Metalloporphyrins, which cannot coordinate the ligands (for example, Cu^{II}OEP), do not form such complexes. Ionic (Cation⁺)•{Co^{II}OEP•(C₆₀⁻)}•(Solvent)_x complexes were obtained even with noncoordinated cations (MQ⁺, TMP⁺) since Co^{II}OEP itself can form the coordination Co–C(C₆₀⁻) bonds. Since only Co^{II}OEP is able to form stable metal–carbon bonds,²³ such complexes cannot be obtained with other metalloporphyrins (ZnOEP, Mn^{II}OEP, and Fe^{II}OEP). The other important condition for the formation of L(C⁺)•M^{II}OEP•C₆₀(C₆₀⁻) complexes is a small size of ligands or cations used (DABCO, TMP⁺, MQ⁺, and MDABCO⁺) since zigzag fullerene chains in **4–11** have only small vacancies. It is interesting that the use of the DMETEP⁺ cation with long –CH₂–CH₂–S–CH₂–CH₃ substituents affords a crystal structure of **12** different from those of **4–11**. Bulky cations cannot be incor-

porated in the structures of such type in contrast to similar $M^{II}TPP-C_{60}$ complexes, which were obtained even with large $Cr(C_6H_6)_2^{+}$ and $TDAE^{+}$ cations.^{4e,f}

The synthesis of a series of complexes allows one for the first time to study coordination modes of DABCO, MDABCO⁺, DMETEP⁺, C_{60} and C_{60}^{*-} to $M^{II}OEP$ and compare their coordination abilities. We showed that neutral DABCO forms shorter $M-N(L)$ bonds (by 0.049–0.055 Å) than the MDABCO⁺ cation and the DMETEP⁺ cation (by 0.214 Å). Therefore, the DMETEP⁺ cation has the weakest coordination ability among the *N*-containing ligands used. Since only one $L(L^+)$ ligand is coordinated to $M^{II}OEP$, $C_{60}(C_{60}^{*-})$ can also be involved in the bonding with $M^{II}OEP$. However, fullerenes and *N*-containing ligands compete in coordinating to $M^{II}OEP$. The analysis of structural data allows us to conclude that fullerenes are essentially weaker ligands than nitrogen containing ones. As a result, the M^{II} atoms display out of the porphyrin plane toward nitrogen and that prevents the coordination of fullerenes to $M^{II}OEP$. For example, the $M \cdots C(C_{60})$ distances in DABCO containing complexes **4** and **5** are longer by 0.16–0.27 Å than those distances in DABCO free complexes **1** and **2**. Similar tendency was found in ionic complexes **6–9**. The smaller is the displacement of the metal(II) atom from the porphyrin plane toward MDABCO⁺ the shorter $M \cdots C(C_{60}^{*-})$ contacts are formed (as in **7**). Larger $M \cdots C(C_{60}^{*-})$ distances (>3 Å) for ZnOEP and Mn^{II}OEP indicate the absence of coordination in **6** and **9** at 100 K. That is consistent with optical and magnetic data. The MQ^+ and TMP^+ cations do not coordinate to $M^{II}OEP$ and that provides the formation of stable $Co-C(C_{60}^-)$ coordination bonds of the 2.266(3)–2.268(1) Å length in **10** and **11**.

Optical and magnetic studies showed that complexes obtained with metalloporphyrins and metalloporphyrins coordinated neutral DABCO ligand have neutral ground state, whereas complexes obtained with the MDABCO⁺ cations can be classified as completely ionic compounds. Complex **12** is an unique example, which contains simultaneously neutral and -1 charged fullerene species. The coordination of the *N*-containing ligands and cations results in essential red shift of the Soret porphyrin band, whereas the coordination of fullerenes and their anions only weakly shifts the Soret band.

Magnetic properties of the complexes range from a diamagnetic behavior of **10** (due to the formation of the $Co-C(C_{60}^-)$ bond), paramagnetic behavior of **9** and **3** with small Weiss temperatures and strong enough antiferromagnetic coupling of spins in **6** and **8**. Complex **6** contains chains of C_{60}^{*-} , and AF interaction of spins is most probably realized namely in these chains. The absence of structural information for **8** does not allow the detailed interpretation of the magnetic data for this complex, which showed the strongest antiferromagnetic coupling of spins.

Acknowledgment. The work was supported by the Russian Science Support Foundation, INTAS YSF 05-109-4653, RFBR Grants N 06-03-32824 and 06-03-91361, Japan-Russia Research Cooperative Program and Grant-in-Aid Scientific Research from the Ministry of Education, Culture, Sports, Science and Technology, Japan (152005019, 21st Century COE).

Supporting Information Available: Crystallographic information files and table of IR spectra data and UV–visible–NIR spectra. This information is available free of charge via the Internet at <http://pubs.acs.org>.

References

- (1) (a) Balch, A. L.; Olmstead, M. M. *Chem. Rev.* **1998**, *98*, 2123–2165. (b) Konarev, D. V.; Lyubovskaya, R. N. *Russ. Chem. Rev.* **1999**, *68*, 19–38. (c) Gotschy, B. *Fullerene Sci. and Technol.* **1996**, *4*, 677–698. (d) Konarev, D. V.; Lyubovskaya, R. N.; Drichko, N. V.; Yudanov, E. I.; Shul'ga, Y. M.; Litvinov, A. L.; Semkin, V. N.; Tarasov, B. P. *J. Mat. Chem.* **2000**, 803–818. (e) Makha, M.; Purich, A.; Raston, C. L.; Sobolev, A. N. *Eur. J. Inorg. Chem.* **2006**, *50*, 7–517. (f) Norret, M.; Makha, M.; Sobolev, A. N.; Raston, C. L. *New J. Chem.* **2008**, *32*, 808–812.
- (2) (a) Olmstead, M. M.; Costa, K.; Maitra, D. A.; Noll, B. C.; Phillips, S. L.; Van Calcar, P. M.; Balch, A. L. *J. Am. Chem. Soc.* **1999**, *121*, 7090–7097. (b) Boyd, P. D. W.; Hodgson, M. C.; Rickard, C. E. F.; Oliver, A. G.; Chaker, L.; Brothers, P. J.; Bolskar, R. D.; Tham, F. S.; Reed, C. A. *J. Am. Chem. Soc.* **1999**, *121*, 10487–10495. (c) Ishii, T.; Aizawa, N.; Yamashita, M.; Matsuzaka, H.; Kodama, T.; Kikuchi, K.; Ikemoto, I.; Iwasa, Y. *J. Chem. Soc., Dalton Trans.* **2000**, 4407–4412. (d) Konarev, D. V.; Neretin, I. S.; Slovokhotov, Y. L.; Yudanov, E. I.; Drichko, N. V.; Shul'ga, Y. M.; Tarasov, B. P.; Gumanov, L. L.; Batsanov, A. S.; Howard, J. A. K.; Lyubovskaya, R. N. *Chem. Eur. J.* **2001**, *7*, 2605–2616. (e) Konarev, D. V.; Kovalevsky, A. Yu.; Li, X.; Neretin, I. S.; Litvinov, A. L.; Drichko, N. V.; Slovokhotov, Y. L.; Coppens, P.; Lyubovskaya, R. N. *Inorg. Chem.* **2002**, *41*, 3638–3646. (f) Ishii, T.; Aizawa, N.; Kanehama, R.; Yamashita, M.; Sugiura, K.; Miyasaka, H. *Coord. Chem. Rev.* **2002**, *226*, 113–124.
- (3) (a) Stevenson, S.; Rice, G.; Glass, T.; Harich, K.; Cromer, F.; Jordan, M. R.; Craft, J.; Hadju, E.; Bible, R.; Olmstead, M. M.; Maitra, K.; Fisher, A. J.; Balch, A. L.; Dorn, H. C. *Nature* **1999**, *401*, 55–57. (b) Olmstead, M. M.; de Bettencourt-Dias, A.; Stevenson, S.; Dorn, H. C.; Balch, A. L. *J. Am. Chem. Soc.* **2002**, *124*, 4172–4173. (c) Zheng, M.; Li, F.; Shi, Z.; Gao, X.; Kadish, K. M. *J. Org. Chem.* **2007**, *72*, 2538–2543.
- (4) (a) Konarev, D. V.; Khasanov, S. S.; Slovokhotov, Y. L.; Saito, G.; Lyubovskaya, R. N. *CrystEngComm.* **2008**, *10*, 48–53. (b) Konarev, D. V.; Khasanov, S. S.; Saito, G.; Otsuka, A.; Lyubovskaya, R. N. *Inorg. Chem.* **2007**, *46*, 7601–7609. (c) Konarev, D. V.; Khasanov, S. S.; Otsuka, A.; Saito, G.; Lyubovskaya, R. N. *J. Am. Chem. Soc.* **2006**, *128*, 9292–9293. (d) Konarev, D. V.; Khasanov, S. S.; Otsuka, A.; Saito, G.; Lyubovskaya, R. N. *Inorg. Chem.* **2007**, *46*, 2261–2271. (e) Konarev, D. V.; Khasanov, S. S.; Otsuka, A.; Yoshida, Y.; Lyubovskaya, R. N.; Saito, G. *Chem. Eur. J.* **2003**, *9*, 3837–3848. (f) Konarev, D. V.; Neretin, I. S.; Saito, G.; Slovokhotov, Y. L.; Otsuka, A.; Lyubovskaya, R. N. *Dalton Trans.* **2003**, 3886–3891. (g) Konarev, D. V.; Khasanov, S. S.; Otsuka, A.; Saito, G.; Lyubovskaya, R. N. *Chem. Eur. J.* **2006**, *12*, 5225–5230.
- (5) Saito, G.; Teramoto, T.; Otsuka, A.; Sugita, Y.; Ban, T.; Kusunoki, M.; Sakaguchi, K. *Synth. Met.* **1994**, *64*, 359–368.
- (6) (a) Konarev, D. V.; Khasanov, S. S.; Saito, G.; Otsuka, A.; Yoshida, Y.; Lyubovskaya, R. N. *J. Am. Chem. Soc.* **2003**, *125*, 10074–10083. (b) Allemand, P.-M.; Khemani, K. C.; Koch, A.; Wudl, F.; Holczer, K.; Donovan, S.; Grüner, G.; Thompson, J. D. *Science* **1991**, *253*, 301–303. (c) Kitagawa, T.; Lee, Y.; Takeuchi, K. *Chem. Commun.* **1999**, 1529–1530.
- (7) Otwinowski, Z. Minor, W. In *Processing of X-ray diffraction data collection in oscillation, Methods in Enzymology*, Eds. Carter, C. W.; Sweet, R. M., Eds.; Academic Press: New York, 1997; p 276.
- (8) Bruker Analytical X-ray Systems, Madison, Wisconsin, U.S.A., 1999.
- (9) Sheldrick, G. M. *SHELX97*; University of Göttingen: Germany, 1997.
- (10) Konarev, D. V.; Kovalevsky, A. Y.; Khasanov, S. S.; Lopatin, D. V.; Umrikhin, A. V.; Saito, G.; Lyubovskaya, R. N. *Cryst. Growth Des.* **2008**, *8*, 1161–1172.
- (11) Rowland, R. S.; Taylor, R. J. *Phys. Chem.* **1996**, *100*, 7384–7391.
- (12) (a) Lee, H. M.; Olmstead, M. M.; Suetsuna, T.; Shimotani, H.; Drago, N.; Cross, R. J.; Kitazawa, K.; Balch, A. L. *Chem. Commun.* **2002**, 1852–1853. (b) Olmstead, M. M.; Bettencourt-Dias, A.; Lee, H. M.; Pham, D.; Balch, A. L. *Dalton Trans.* **2003**, 322, 7–3232.
- (13) (a) Mikami, S.; Sugiura, K.; Asato, E.; Maeda, Y.; Sakat, Y. *The Proceedings of the Conference "The 19th Fullerene General Symposium"*, Kiryu, Japan, July 27–28, 2000; p 40. (b) Evans, D. R.; Fackler, N. L. P.; Xie, Z.; Rickard, C. E. F.; Boyd, P. D. W.; Reed, C. A. *J. Am. Chem. Soc.* **1999**, *121*, 8466–8474. (c) Ishii, T.; Kanehama, R.; Aizawa, N.; Yamashita, M.; Matsuzaka, H.; Sugiura, K.; Miyasaka, H.; Kodama, T.; Kikuchi, K.; Ikemoto, I.; Tanaka, H.; Marumoto, K.; Kuroda, S.-I. *J. Chem. Soc., Dalton Trans.* **2001**, 2975–2980.
- (14) Hu, C.; Noll, B. C.; Schulz, C. E.; Scheidt, W. R. *J. Am. Chem. Soc.* **2005**, *127*, 15018–15019.
- (15) Picher, T.; Winkler, R.; Kuzmany, H. *Phys. Rev. B* **1994**, *49*, 15879–15889.
- (16) (a) Konarev, D. V.; Neretin, I. S.; Litvinov, A. L.; Drichko, N. V.; Slovokhotov, Y. L.; Lyubovskaya, R. N.; Howard, J. A. K.; Yufit, D. S. *Cryst. Growth Des.* **2004**, *4*, 643–646. (b) Litvinov, A. L.;

- Konarev, D. V.; Kovalevsky, A. Y.; Coppens, P.; Lyubovskaya, R. N. *Cryst. Growth Des.* **2005**, *5*, 1807–1819.
- (17) (a) Radonovich, L. J.; Bloom, A.; Hoard, S. L. *J. Am. Chem. Soc.* **1972**, *94*, 2073–2078. (b) Hu, C.; Au, J.; Noll, B. C.; Schulz, C. E.; Scheidt, W. R. *Inorg. Chem.* **2006**, *45*, 4177–4185.
- (18) Marumoto, K.; Takahashi, H.; Tanaka, H.; Kuroda, S.; Ishii, T.; Kanehama, R.; Aizawa, N.; Yamashita, M. *J. Phys.: Condens. Matter* **2004**, *16*, 8753–8762.
- (19) Reed, C. A.; Bolskar, R. D. *Chem. Rev.* **2000**, *100*, 1075–1120.
- (20) (a) Kirner, J. F.; Reed, C. A.; Scheidt, W. R. *J. Am. Chem. Soc.* **1977**, *99*, 2557–2563. (b) Reed, C. A.; Kouba, J. K.; Grimes, C. J.; Cheung, S. K. *Inorg. Chem.* **1978**, *17*, 2666–2670. (c) Scheidt, W. R.; Hatano, K.; Rupprecht, G. A.; Piciulo, P. L. *Inorg. Chem.* **1979**, *18*, 292–299.
- (21) Mulliken, R. S.; Person, W. B. *Molecular Complexes*; Academic Press: New York, 1969.
- (22) Furhop, J. H.; Kadish, K. M.; Davis, D. G. *J. Am. Chem. Soc.* **1973**, *95*, 5140–5147.
- (23) Rossi, M.; Glusker, J. P.; Randaccio, L.; Summers, M. F.; Toscano, P. J.; Marzilli, L. G. *J. Am. Chem. Soc.* **1985**, *107*, 1729–1738.

CG8010184